

efficiently. No EPR evidence for the species characteristic of activated bleomycin nor of the compound I type species of HRP could be found with Fe(III)-bleomycin A₂ in the presence of iodosobenzene. This is consistent with the report that thymine is not released from DNA treated with Fe(III)-bleomycin plus iodosobenzene.¹⁵ (Thymine is readily released from DNA treated with O₂-activated Fe(II)-bleomycin or H₂O₂-activated Fe(III)-bleomycin.^{11,35})

Fe(III)- and Cu(II)-bleomycin A₂ are susceptible to damage by the oxidant, and experiments show a rapid reaction between iodosobenzene and metal-free bleomycin A₂, leading to a loss of metal binding capacity. Also, Fe(III) forms an EPR-silent complex when iodosobenzene is added to Fe(III)-bleomycin A₂, which suggests removal of the metal from the drug complex.

Iodosobenzene activation of Fe(III) in some porphyrin models is described in several accounts.^{5,6,17-20,32} However, this reagent is not a benign oxygen surrogate in reactions with bleomycin. The use of iodosobenzene and related hypervalent iodine complexes in synthetic organic chemistry has been reviewed.³³ Its ability to cleave glycols (in a reaction analogous to lead tetraacetate oxidations) as well as its reactivity toward carboxylic acids, amides, and other functional groups could interfere with its usefulness as an activation surrogate in the case of bleomycin. The reports of epoxidations and other reactions using Fe(III)- and Cu(II)-bleomycin with iodosobenzene, considering the long incubations generally employed, must be viewed with caution since the drug molecule as well as the Fe(III)-drug complex breaks down rapidly. Recent reports of relatively effective and stereospecific catalysis of epoxidation by iodosobenzene in the presence of metal salts (Fe, Cu),^{21,23} binuclear Cu(II) complexes,^{22,34} or Zn(II)-bleomycin²¹ suggest that the experimental data gathered with metallobleomycins could reflect catalysis by complexes unrelated to a putative hypervalent iron-bleomycin complex.

The disappearance of the EPR signal due to Fe(III)-bleomycin in mixtures containing iodosobenzene could be interpreted as evidence for the formation of a nonparamagnetic hypervalent iron-oxo complex, though the finding of similar behavior with Fe(III) in the absence of the bleomycin ligand, the finding that the drug cannot bind Fe(III) in the presence of iodosobenzene, and the absence of EPR signals due to other perferryl complexes argue against the notion that the loss of EPR signal represents activation of iron bleomycin.

Acknowledgment. J.P. is the recipient of United States Public Health Service Grant GM-40168.

- (31) Magliozzo, R. S. Unpublished observations.
 (32) Castellino, A. J.; Bruice, T. C. *J. Am. Chem. Soc.* **1988**, *110*, 158-162.
 (33) Vargolis, A. *Chem. Soc. Rev.* **1981**, *10*, 377.
 (34) Fan Tai, A.; Margerum, L. D.; Valentini, J. S. *J. Am. Chem. Soc.* **1986**, *108*, 5006-5008.
 (35) A reviewer has suggested that activated bleomycin is probably a ferric-peroxy complex and that the species responsible for DNA cleavage or for the oxidation of small molecules may in fact be a different iron-oxo species formed subsequent to O-O bond cleavage, this second species being the analogue of activated cytochrome P-450. We suggest that this species, if it maintains the perferryl oxidation state of the original activated bleomycin and forms via heterolytic cleavage of the peroxide, should also have odd electron spin and exhibit an EPR spectrum. There is no evidence, however, that bleomycin forms a second EPR-active species after activation. Alternatively, a homolytic O-O cleavage subsequent to the formation of a ferric-peroxy complex¹¹ could give a ferric iron-oxo radical pair that would be EPR silent. The kinetics of decay of activated bleomycin, as stated above, argues against any intermediate between activated bleomycin and the species that attacks DNA. The reviewer further suggested that iodosobenzene generates a complex from Fe(III)-bleomycin that is equivalent to the purported species formed after bleomycin activation and that this secondary complex is "the species ultimately responsible for the observed chemistry of Fe-bleomycin". Since iodosobenzene does not activate Fe(III)-bleomycin¹⁵ for the type of DNA cleavage characteristic of oxygen or peroxide activation in which thymine is released,¹¹ the interactions cannot be related. It should be noted that chain breakage of SV 40 DNA has been observed with Cu(II)- or Fe(III)-bleomycin in the presence of 100-fold excesses of iodosobenzene: Ehrenfeld, G. M.; Rodriguez, L. O.; Hecht, S. M.; Chang, C.; Basus, V. J.; Oppenheimer, N. J. *Biochemistry* **1985**, *24*, 81-92.

Contribution from the Institut für Physikalische und Theoretische Chemie and Physikalisches Institut, Abt. II, University of Erlangen-Nürnberg, D-8520 Erlangen, West Germany, and The Open University, Belfast BT7 1SU, Northern Ireland

Detailed Study of the Quintet \rightleftharpoons Singlet Spin Transition in Bis(selenocyanato)bis(2,2'-bi-2-thiazoline)iron(II)

E. König,^{*1a} G. Ritter,^{1b} J. Dengler,^{1b} and J. Nelson²

Received June 13, 1988

Iron(II) complexes of the series [FeL₂X₂], where L = 2,2'-bi-2-thiazoline (bt) or an alkyl-substituted derivative thereof and X = NCS or NCSe, are known to exhibit thermally induced spin-state transitions in the solid state.³ Thus the high-spin (HS, S = 2) \rightleftharpoons low-spin (LS, S = 0) transition in [Fe(bt)₂(NCS)₂] has been the subject of rather detailed investigations⁴ including an attempt at the rationalization of the mechanism of the transition on the basis of the domain formalism.⁵ On the other hand, more detailed studies are lacking for the spin-state transition in the analogous selenocyanato complex [Fe(bt)₂(NCSe)₂]. The transition in this complex is of particular interest since it is one of the most abrupt ones ever encountered for compounds of iron(II).

In the present paper, we report therefore studies of the HS \rightleftharpoons LS transition in [Fe(bt)₂(NCSe)₂] employing the ⁵⁷Fe Mössbauer effect and X-ray powder diffraction.

Experimental Section

Materials. Samples of [Fe(bt)₂(NCSe)₂] were prepared as described elsewhere.³ The purity of the substance was checked by elemental analysis, magnetic measurements, and ⁵⁷Fe Mössbauer spectroscopy.

Mössbauer Spectroscopy. The ⁵⁷Fe Mössbauer spectra were measured with a spectrometer consisting of a constant-acceleration electromechanical drive and a Nuclear Data ND 2400 multichannel analyzer operating in the multiscaling mode. The source used consisted of 50-mCi ⁵⁷Co in rhodium at room temperature, the calibration being effected with a 25- μ m iron foil absorber. All velocity scales and isomer shifts are referred to the iron standard at 298 K. For conversion to the sodium nitroprusside scale, add +0.257 mm s⁻¹. Variable-temperature measurements between 80 and 300 K were performed by using a custom-made cryostat, the temperature being monitored by means of a calibrated iron vs constantan thermocouple and a cryogenic temperature controller (Thor Cryogenics Model E 3010-II). The temperature stability was about \pm 0.10 K. The Mössbauer spectra were corrected for nonresonant background of the γ -rays and were least-squares fitted to Lorentzian line shapes. In order to determine values of the relative effective thickness t_i from the area of each individual Mössbauer line i , the experimental data were fitted in terms of the general expression of the Mössbauer spectrum.⁶ The effective thicknesses for the quadrupole doublets of the high-spin (HS) and low-spin (LS) phases are then determined according to

$$t_{\text{HS}} = (t_1 + t_2)_{\text{HS}} = dn_{\text{HS}}f_{\text{HS}}$$

$$t_{\text{LS}} = (t_1 + t_2)_{\text{LS}} = d(1 - n_{\text{HS}})f_{\text{LS}} \quad (1)$$

In eq 1, $d = N\beta\delta\sigma_0$ where N is the number of iron atoms per unit volume, β the isotopic abundance, δ the absorber thickness, and σ_0 the resonance cross section. In addition, n_{HS} is the HS fraction, with f_{HS} and f_{LS} being the Debye-Waller factors of the two phases.

X-ray Diffraction. Measurements of X-ray powder diffraction at variable temperatures were obtained with a Siemens counter diffractometer equipped with an Oxford Instruments CF108A continuous-flow cryostat and liquid nitrogen as coolant. The diffractometer was used in

- (1) (a) Institut für Physikalische und Theoretische Chemie, University of Erlangen-Nürnberg. (b) Physikalisches Institut, Abt. II, University of Erlangen-Nürnberg.
 (2) The Open University.
 (3) Bradley, G.; McKee, V.; Nelson, S. M.; Nelson, J. *J. Chem. Soc., Dalton Trans.* **1978**, 522.
 (4) König, E.; Ritter, G.; Irlner, W.; Nelson, S. M. *Inorg. Chim. Acta* **1979**, *37*, 169.
 (5) Müller, E. W.; Spiering, H.; Gütlich, P. *J. Chem. Phys.* **1983**, *79*, 1439.
 (6) König, E.; Ritter, G.; Waigel, J.; Goodwin, H. A. *J. Chem. Phys.* **1985**, *83*, 3055.

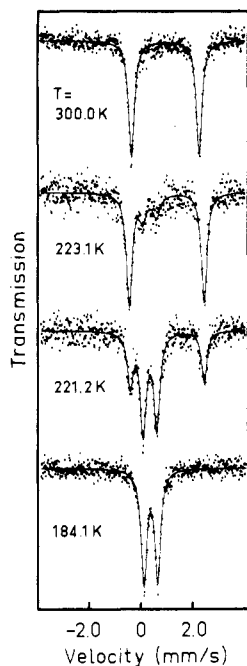


Figure 1. ^{57}Fe Mössbauer spectra of $[\text{Fe}(\text{bt})_2(\text{NCSe})_2]$ at 300.0, 223.1, 221.2, and 184.1 K. The measurements have been performed for decreasing temperature ($T_c^{\downarrow} \approx 221.3$ K).

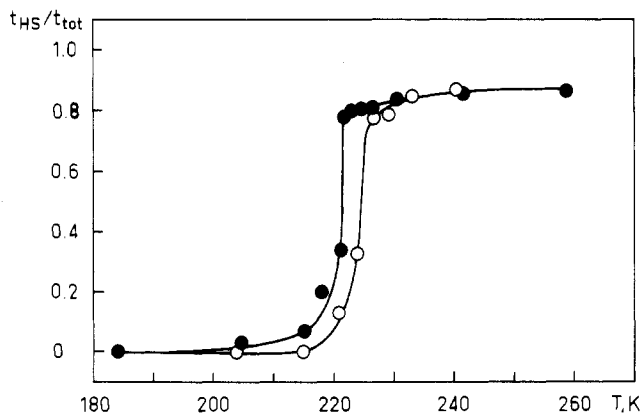


Figure 2. Temperature dependence of the relative effective thickness $t_{\text{HS}}/t_{\text{total}}$ of the Mössbauer effect for increasing (O) and decreasing (●) temperature ($T_c^{\downarrow} \approx 224.9$; $T_c^{\uparrow} \approx 221.3$ K).

the mode of step scanning, the angular steps having been 0.005° in terms of 2θ . Cu $K\alpha$ radiation was used, and a temperature stability of ± 0.1 K was achieved. The resulting pulses were stored in an Elscint MEDA 10 multichannel analyzer and displayed as such.

Results

The ^{57}Fe Mössbauer effect for the complex $[\text{Fe}(\text{bt})_2(\text{NCSe})_2]$ has been measured between 92 and 300 K for both increasing and decreasing temperatures, the results being collected in Table I. In addition, Mössbauer spectra at 300.0, 223.1, 221.2, and 184.1 K are illustrated in Figure 1 for decreasing temperatures. Figure 2 shows the relative effective thickness $t_{\text{HS}}/t_{\text{total}}$ derived from the Mössbauer spectra as a function of temperature. It is evident that the transition is associated with a pronounced hysteresis, the transition temperatures being $T_c^{\downarrow} \approx 221.3$ K and $T_c^{\uparrow} \approx 224.9$ K for decreasing and increasing temperature, respectively.

The temperature dependence of X-ray powder diffraction has been studied between 77 and 300 K. Figures 3 and 4 show the results for decreasing temperature, the region of Bragg angles between 6.00 and 8.20° being displayed in Figure 3 with that of Bragg angles between 9.00 and 10.40° displayed in Figure 4. It is clearly seen that there is a pronounced change of peak profiles between the temperatures of 222.0 and 220.0 K. The results for increasing temperature show a corresponding change of peak

Table I. ^{57}Fe Mössbauer Effect Parameters for $[\text{Fe}(\text{bt})_2(\text{NCSe})_2]^a$

T , K	$\Delta E_Q^{\text{HS},b}$ mm s $^{-1}$	$\delta_{\text{HS}}^{\text{IS},c}$ mm s $^{-1}$	$\Delta E_Q^{\text{LS},b}$ mm s $^{-1}$	$\delta_{\text{LS}}^{\text{IS},c}$ mm s $^{-1}$	$t_{\text{HS}}/t_{\text{total}}^d$
300.0	2.60	+0.974			1.00
258.7	2.75	+1.00	0.65 ± 0.05	$+0.46 \pm 0.03$	0.87
241.6	2.82	+1.01	0.69 ± 0.04	$+0.45 \pm 0.02$	0.86
230.5	2.88	+1.00	0.55 ± 0.03	+0.35	0.84
226.3	2.87	+1.01	0.61 ± 0.03	+0.36	0.81
224.6	2.88	+1.01	0.57 ± 0.03	+0.37	0.81
223.1	2.89	+1.02	0.51 ± 0.03	+0.36	0.80
221.6	2.88	+1.02	0.60 ± 0.02	+0.38	0.78
221.2	2.86	+1.02	0.53	+0.35	0.34
218.1	2.89 ± 0.02	+1.02	0.53	+0.35	0.20
215.1	2.87 ± 0.05	$+1.02 \pm 0.02$	0.52	+0.35	0.07
204.8	2.92 ± 0.11	$+1.00 \pm 0.05$	0.53	+0.35	0.03
184.1			0.53	+0.36	0
203.7			0.53	+0.35	0
214.8			0.53	+0.36	0
220.7	2.86 ± 0.05	$+0.99 \pm 0.02$	0.52	+0.35	0.13
223.9	2.86 ± 0.02	+1.01	0.52	+0.35	0.33
226.5	2.89	+1.02	0.59 ± 0.03	+0.36	0.78
229.1	2.84	+1.00	0.55 ± 0.03	+0.37	0.79
233.0	2.83	+1.00	0.58 ± 0.05	$+0.41 \pm 0.02$	0.85
240.3	2.82	+1.01	0.70 ± 0.04	$+0.36 \pm 0.02$	0.87

^aData are listed in the order of measurement. ^bExperimental uncertainty is smaller than or equal to ± 0.01 mm s $^{-1}$ except where stated. ^cIsomer shifts δ^{IS} are listed relative to that of natural iron at 298 K; experimental uncertainty is smaller than or equal to ± 0.01 mm s $^{-1}$ except where stated. ^dExperimental uncertainty ≤ 0.01 mm s $^{-1}$.

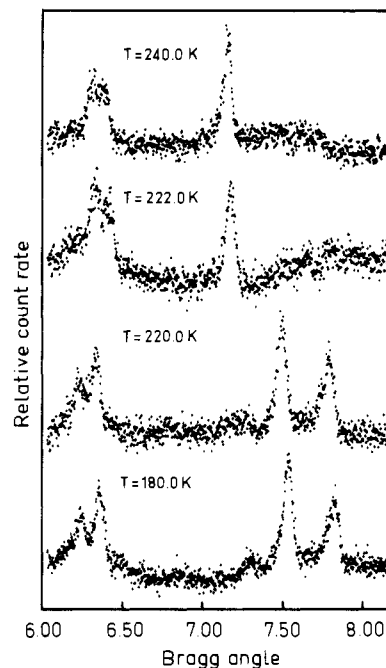


Figure 3. X-ray powder diffraction peak profiles of $[\text{Fe}(\text{bt})_2(\text{NCSe})_2]$ for Bragg angles between 6.00 and 8.20° at 240.0, 222.0, 220.0, and 180.0 K. The data are for decreasing temperature.

profiles between the temperatures of 225.0 and 227.0 K.

Discussion

The Mössbauer spectra between 92 and 300 K are clear evidence of the HS ($S = 2$) \rightleftharpoons LS ($S = 0$) transition in the solid complex $[\text{Fe}(\text{bt})_2(\text{NCSe})_2]$. The observation of a thermal hysteresis of width $\Delta T_c = 3.6$ K demonstrates that the transition is thermodynamically first order. This conclusion is well supported by the results of X-ray powder diffraction measurements, which show that the diffraction pattern of the HS state is replaced by that of the LS state on cooling and vice versa on heating. The temperature at which the transformation from the HS to the LS pattern (or vice versa) occurs is lower for a sample undergoing cooling than for one undergoing heating. This shows that a hysteresis similar to that in the Mössbauer effect is found for X-ray diffraction. In fact, the temperatures of 222.0 and 220.0 K for

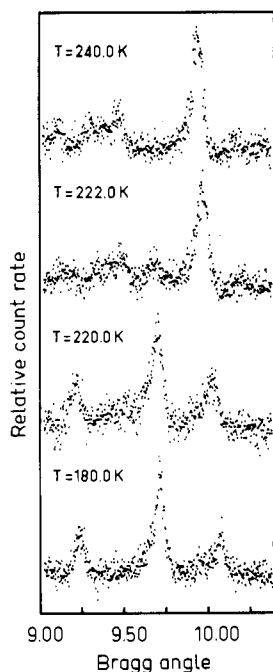


Figure 4. X-ray powder diffraction peak profiles of $[\text{Fe}(\text{bt})_2(\text{NCSe})_2]$ for Bragg angles between 9.00 and 10.40° at 240.0 , 222.0 , 220.0 , and 180.0 K. The data are for decreasing temperature.

decreasing temperatures encompass the transition temperature $T_c \approx 221.3$ K quite well (see Figures 3 and 4), those of 225.0 and 227.0 K for increasing temperatures (not displayed here) being only slightly offset from the value $T_c \approx 224.9$ K derived from the Mössbauer spectra. It is obvious, on the basis of previous studies,^{7,8} that the X-ray powder diffraction at T_c will comprise the patterns of both the HS and LS phases in equal proportion. Due to the very sharp nature of the transition in the present substance, the construction of such a diffraction pattern is, however, difficult to accomplish. First of all, the observed hysteresis requires that, in approaching T_c , the direction of temperature variation should not be reversed. Second, differences of temperature calibration will result in slightly different T_c values for Mössbauer effect and X-ray diffraction measurements.

In more general terms, the observation of two different diffraction patterns for a discontinuous spin-state transition indicates that the two phases involved are characterized by different unit cell parameters.⁷ These unit cells correspond to the discrete molecular structures associated with the HS and LS states of the $[\text{Fe}(\text{bt})_2(\text{NCSe})_2]$ complex that are participating in the transition.

The findings are well in line with the results found for a number of first-order spin-state transitions in compounds of iron(II).⁸ In particular, the transition seems to be closely related to that observed for the compound $[\text{Fe}(\text{bt})_2(\text{NCS})_2]$ containing the same ligand.^{3,4} As indicated by the change of the effective magnetic moment,³ the transition in $[\text{Fe}(\text{bt})_2(\text{NCSe})_2]$ is almost as abrupt as that observed for the thiocyanato complex, whereas the hysteresis width is considerably lower, $\Delta T_c = 3.6$ vs 9.5 K for $[\text{Fe}(\text{bt})_2(\text{NCS})_2]$.⁴

In order to investigate a possible trapping of the HS species, the effect of rapid cooling of a sample of $[\text{Fe}(\text{bt})_2(\text{NCSe})_2]$ has been investigated by the Mössbauer effect. However, no unusual behavior has been observed. Apparently, the transition in this compound is reversible and fast, at least under the conditions imposed by the experiment.

Acknowledgment. We appreciate financial support by the Deutsche Forschungsgemeinschaft, Bonn, West Germany.

Registry No. $[\text{Fe}(\text{bt})_2(\text{NCSe})_2]$, 67903-90-6.

Contribution from the Institute of Solid State Chemistry, Siberian Academy of Science of the USSR, 630091, Novosibirsk 91, Derzhavina 18, USSR, Nankai University, Weijin Road 94, Tian-jin, People's Republic of China, and Laboratoire de Chimie du Solide du CNRS, Université de Bordeaux I, 351 cours de la Libération, 33405 Talence Cedex, France

The Ternary System Mg-Co-H

E. J. Ivanov,[†] I. Konstanchuk,[†] A. Stepanov,[†] Yan Jie,[‡] M. Pezat,[§] and B. Darriet*[§]

Received February 3, 1988

In the scope of a research program for preparing and characterizing new hydrogen storage materials containing Mg and 3d metal elements, two ternary hydrides, Mg_2FeH_6 ^{1,2} and Mg_2CoH_5 ,³ have been detected recently. Zolliker et al.³ have prepared Mg_2CoH_5 and its deuteride by a sintering technique at temperatures between 620 and 770 K and under a hydrogen (or deuterium) pressure of 4 – 6 MPa. These compounds are black crystalline solids. X-ray and neutron powder diffraction data recorded at room temperature suggested, according to the authors, a tetragonally distorted CaF_2 -type metal atom structure. They specified that the structure transforms at 488 (5) K into a disordered cubic-symmetry modification. They pointed out the existence of another ternary hydride as well, which, however, was not further investigated. In the present paper we report new results that we have obtained in studying the ternary system Mg-Co-H.

Experimental Procedure

Several samples were prepared as follows. Magnesium and cobalt powders in a 2:1 atomic ratio were mixed for 2–3 days in a ball mill. These mixtures were pressed into pellets under 500 -MPa pressure and placed in a steel autoclave. They were hydrided for several days at temperatures and pressures selected with reference to the phase diagram. Other samples were prepared by mechanical alloying in a high-energy planetary ball mill (600 m/s²) as described elsewhere.⁴ Mechanically alloyed samples were not pressed into pellets before reaction with hydrogen under the chosen conditions. The reaction products consisted of small amounts of MgH_2 , Mg, and Co in addition to a ternary hydride. The Mg and MgH_2 impurities were removed by treatment in 1,2-dibromoethane in a way described elsewhere.³ The Co content was checked by magnetic susceptibility measurements.

The composition of the purified samples has been determined chemically by complexometric titration with EDTA and by electron microprobe analysis ("Camebax Micro", Cameca).

The pressure-composition isotherms were determined on unpurified and purified samples by hydrogen desorption.

X-ray powder diffraction data were recorded by using $\text{Cu K}\alpha$ radiation. The electrical conductivity was measured for the pressed pellets under 500 -MPa pressure in a stainless steel reactor under hydrogen pressure. The reactor design allows us to use only a dc two-electrode cell. A Model DSC-111 "Setaram" instrument was used for the thermal analysis experiments.

Results and Discussion

The magnesium-cobalt mechanical alloys begin to absorb hydrogen at pressures below the equilibrium pressure of MgH_2 . In other words the ternary hydrides of magnesium and cobalt form by direct combination of Mg, Co, and H_2 .

Figure 1 shows several desorption isotherms corresponding to unpurified samples that had been previously hydrided at 660 K under $P_{\text{H}_2} = 4$ MPa. They exhibit three plateau pressures. The upper one corresponds to the decomposition of MgH_2 . This result is confirmed by the calculated enthalpy and entropy values

$$\Delta H^\circ = -75 \pm 1 \text{ kJ (mol of H}_2\text{)}^{-1}$$

$$\Delta S^\circ = -135 \pm 2 \text{ J K}^{-1} \text{ (mol of H}_2\text{)}^{-1}$$

which are very close to those found by Stampfer for MgH_2 ⁵ ($\Delta H^\circ = -74.3$ kJ (mol of H_2)⁻¹ and $\Delta S^\circ = -134.9$ J K⁻¹ (mol of H_2)⁻¹).

[†] Siberian Academy of Science of the USSR.

[‡] Nankai University.

[§] Université de Bordeaux I.

(7) König, E. *Prog. Inorg. Chem.* **1987**, *35*, 527.

(8) König, E.; Ritter, G.; Kulshreshtha, S. K. *Chem. Rev.* **1985**, *85*, 219.